Continental Shelf Research 37 (2012) 15–25

Contents lists available at SciVerse ScienceDirect

Continental Shelf Research

journal homepage: www.elsevier.com/locate/csr

Research papers

Phytoplankton phenology and production around Iceland and Faroes

Li Zhai [a,*], Kristinn Gudmundsson [b], Peter Miller [c], Wenjun Peng [a], Hafsteinn Guðfinnsson [b], Høgni Debes [d], Hjálmar Hátún [d], George N. White III [a], Rafael Hernández Walls [e], Shubha Sathyendranath [c], Trevor Platt [c]

[a] Bedford Institute of Oceanography, Canada
[b] Marine Research Institute, Iceland
[c] Plymouth Marine Laboratory, UK
[d] Faroe Marine Research Institute, Faroe Islands
[e] UABC, Km 103, Carr. Tij.-Ens., Ensenada, Baja California, Mexico

ARTICLE INFO

Article history:
Received 31 May 2011
Received in revised form
19 January 2012
Accepted 21 January 2012
Available online 4 February 2012

Keywords:
Phytoplankton
Primary production
Phenology
Iceland
Faroes

ABSTRACT

Phytoplankton phenology and primary production were examined in the Iceland–Faroe region through synthesis of all available data, both *in situ* and remotely sensed. In the Arctic water, the early onset of stratification in spring gave rise to the rapid shallowing of the mixed layer and triggered the earlier spring bloom north of Iceland, whereas the weakly stratified water-column in the Atlantic water and associated deep mixed layer delayed the spring bloom south of Iceland. The protocol (Nearest Neighbor Method, NNM) developed by Platt et al. (2008) was used to estimate the daily, water-column primary production from ocean color data. The key element of the procedure is an archived database, including (in this implementation) 505 sets of parameters of photosynthetic–light curves and 197 vertical profiles of chlorophyll around Iceland–Faroe region. The spatial structure in the climatology of annual primary production determined in this way was consistent with observations made by the simulated *in situ* method using ships as a platform, but, inevitably, the fields produced from the remotely sensed data were smoother. The annual primary production estimated by the NNM method overestimates the (much more sparse) data for *in situ* production by 50% on average. We examined the relative errors in the estimation of primary production that would arise from ignorance of the non-uniformity in the biomass profile. The vertically uniform model tended to underestimate the annual primary production by about 36% compared with the non-uniform model in a spectral calculation.

1. Introduction

Oceanographically, the Iceland–Faroe area is complex, and may be partitioned according to hydrographic understanding into six regions (Fig. 1). The warm and saline Atlantic water is carried by the North Atlantic Current and the Irminger Current approaching the Iceland Shelf from south and west. The cold and fresh Arctic water flows as the East Icelandic Current north of the Iceland Shelf. The Polar water feeds the East Greenland Current. The Mixed water is the recirculated Atlantic water and is much influenced by the Arctic water masses. The two shelf regions over northeast and southwest of Iceland are defined following 500-m depth contours. However, a detailed frontal analysis (Fig. 2) showed that this partition is a dynamic one: the boundaries between regions fluctuate from one time to another. It is worth noting that changes in relative influence of Polar water and Atlantic water, a branch from the Irminger Current west of Iceland to the shelf north of Iceland, make the northeast Iceland region extremely variable from one year to another. The environmental conditions for the shelf water north of Iceland have been characterized as cold (Polar water), warm (Atlantic water) or something in between (Arctic water) according to the results of annual hydrographical measurements north of Iceland, and these variations apparently influence the primary production (Gudmundsson, 1998; Anon, 2008).

Previous estimates of annual primary production in the region were made solely on the basis of simulated *in situ* experiment conducted at sea (Thordardottir, 1994). Although the network of stations occupied is unusually rich (Fig. 9), and the data accumulated over many years, the resultant map of estimated annual primary production is vulnerable to bias from extreme values at particular stations. The advantages of combining the ship data with remotely-sensed data on visible spectral radiometry (ocean color), for which the principal deliverable is concentration of chlorophyll, include superior spatial resolution and better temporal coverage. Until now, the operational estimation of daily

* Corresponding author. Tel.: +1 902 4269857.
E-mail address: lzhai@phys.ocean.dal.ca (L. Zhai).

0278-4343/$ - see front matter © 2012 Elsevier Ltd. All rights reserved.
doi:10.1016/j.csr.2012.01.013

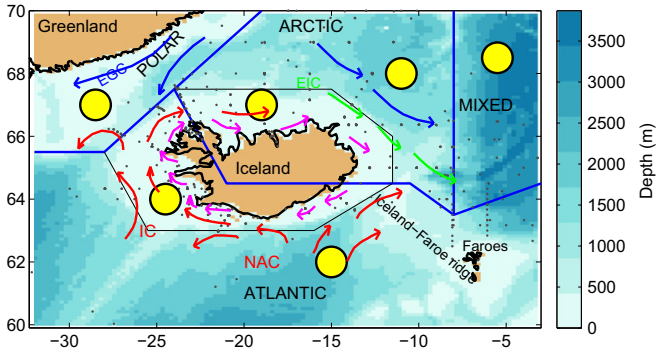

Fig. 1. Bathymetry and circulation around Iceland. Based on the knowledge of the local water masses, the study area is divided into four oceanic regions by blue lines, and three shelf regions by black lines: Polar, Arctic, Mixed, Atlantic, northern Iceland Shelf, and southern Iceland Shelf. The circulation around Iceland is summarized as follows: East Greenland Current (EGC), East Icelandic Current (EIC), North Atlantic Current (NAC), Irminger Current (IC) and coastal currents (purple arrows). The yellow circles show the areas averaged for the representation of region-specific properties. The sampling stations (black dots) at which the photosynthetic–light experiments are made from years 1981 to 2009 are superimposed. Modified from Gudmundsson et al. (2009).

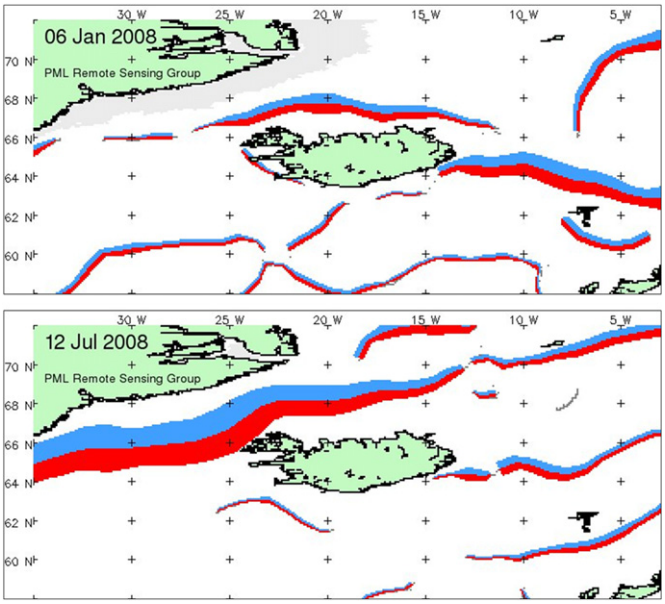

Fig. 2. Examples of 7-day composite front maps from merged microwave/infrared SST data (9 km resolution) around Iceland (Miller, 2009). Red and blue colors indicate the warm and cold sides. The line width indicates the strength of the front.

primary production from remote sensing using a formal parameter assignment protocol, such as the Nearest Neighbor Method (NNM, Platt et al., 2008) has not been made for the Iceland–Faroe area.

The information on phytoplankton and primary production can be utilized to facilitate ecosystem-based management (Platt et al., 2007), such as exploring the correlations between phytoplankton growth and the fate of the primary production through the food chain and casting light on the principal causes of variations in harvestable marine organisms (Astthorsson et al., 2007). The objectives of this study are to estimate primary production for the Iceland–Faroe region from remotely sensed data on ocean color and available ship data, and to characterize the phytoplankton phenology.

2. Material and methods

Most of the *in situ* results used were collected over many years by the Marine Research Institute, Iceland under the leadership of Thorunn Thordardottir (1925–2007). Without this investment, we would not have been able to carry out the work reported here.

2.1. Simulated in situ primary production

Simulated *in situ* primary production was measured by the ^{14}C technique (Steemann Nielsen, 1952). The procedure (Strickland and Parson, 1972; Parsons et al., 1984) was to take water samples, inoculate 50 ml aliquots in clear glass bottles with known activity of radioactive bicarbonate (2−4 μCi per sample) and expose them to a range of light intensities in a temperature regulated incubator. The incubation temperature was adjusted to the *in situ* temperature of the seawater at the time of sampling, and the samples were usually incubated for 4 h (accepting 2–6 h). Water samples from 0, 10, 20 and 30 m were sampled at each station, if possible, and the entire contents of each subsample were filtered onto a cellulose membrane filter (0.2 m) within an hour after incubation. The filters were then dried, in clamps, and exposed to concentrated HCl fumes for five minutes before measuring the radioactivity, using GM-counters. Each filter was counted from both sides in order to correct for varying penetration of ^{14}C into the filters (Theodorsson, 1975) in the calculations of total dpm per filter (Theodorsson, 1984). The primary productivity in mg C m^{-3} h^{-1} was calculated for each sample (Strickland and Parson, 1972), integrated through the water column and converted to the daily rate in mg C m^{-2} day^{-1} to get the daily water column production according to a regional adaptation of the original equation of Steemann Nielsen. The data from years 1958 to 1982 were combined to estimate the annual production from a series of seasonal averages of daily production (Thordardottir, 1994).

2.2. Environmental data

The monthly climatological fields of chlorophyll concentration, sea-surface temperature (SST), cloud cover and photosynthetic available light (PAR) for the Iceland–Faroe area were computed from satellite data between year 1998 and 2007, and mapped onto a 0.1° lat × 0.25° lon grid. The satellite data used are global archives, including the 9-km SeaWiFS level-3 binned monthly-averaged chlorophyll concentration and PAR (http://oceancolor.gsfc.nasa.gov/), the 4-km AVHRR Pathfinder monthly SST (http://www.nodc.noaa.gov/SatelliteData/pathfinder4km/), and 1° SSM/I monthly cloud cover (Ferraro et al., 1996). The primary production model is forced by the climatological biomass and irradiance fields, and the inputs of the NNM are climatological biomass and SST. To determine the onset of phytoplankton blooms, we constructed the 8-day climatology of chlorophyll concentration from the 9-km SeaWiFS level-3 binned daily files, since the monthly resolution cannot well characterize a bloom with a duration of several weeks. We have established 8-day climatological time series of chlorophyll representative for the four oceanic and two shelf provinces (Fig. 1). The locations for each time series were chosen to be away from the boundaries between provinces and the time series were averaged within a 50 km radius of the center. The satellite chlorophyll data are not available before March and after October for the study area, due to the low sun zenith angle.

The mixed layer depth is derived from the hydrographic measurements archived by the World Ocean Database 2009 (Boyer et al., 2009). The raw data of temperature and salinity for each month were averaged on a 2.5° Lat × 10° Lon grid and were binned vertically into depth segments of 5 m. The potential density is then calculated from the gridded temperature and

salinity climatologies, and is used to compute the mixed layer depth, defined as the depth at which the potential density changes by 0.05 kg m^{-3} from the sea surface density.

2.3. Parameters of photosynthetic–light curve and biomass profile

The photosynthesis–light experiments were carried out from years 1981 to 2009 and at stations shown in Fig. 1. The water samples were collected from the surface layer and treated according to Parsons et al. (1984). Assimilation of carbon was measured in 13 subsamples at six different light intensities and in dark after 2–4 h in temperature-regulated incubator (Gudmundsson and Valsdóttir, 2004), according to the radioactive carbon technique (Parsons et al., 1984). The chlorophyll *a* concentration, as well as water temperature, was measured for each sample. The photosynthetic parameters, assimilation number (P_m^B) and initial slope (α^B), were derived from photosynthesis–light (*P–I*) curves using the functional form introduced by Jassby and Platt (1976) and Platt et al. (1980). The procedure is to fit the data to the three-parameter function in Platt et al. (1980), using the generalized non-linear least squares method (gnls implemented in the R language). If the fitting is not successful, the data are then fitted to the tanh function in Jassby and Platt (1976). In cases where both equations fit the *P–I* curves well, the results of P_m^B and α^B from both equations were compared, and the differences were not statistically significant from zero. We obtained 505 sets of photosynthetic parameters after excluding values lying outside the range of mean $\pm$ 3 std and deeper than 20 m.

The chlorophyll profiles, collected between 1990 and 2009, were fitted to the function defined in Platt et al. (1988) for parameter estimation with the following form:

$$B(z) = B_0 + \frac{h}{\sigma\sqrt{2\pi}} \exp\left[-\frac{(z-z_m)^2}{2\sigma^2}\right]. \quad (1)$$

Here B_0 (mg m^{-3}) is the background chlorophyll concentration, h (mg m^{-2}) determines the total biomass above the background, σ (m) controls the thickness of the peak and z_m (m) is the depth of the chlorophyll maximum. The optimal values of four parameters were found using the non-linear least squares method. The height H (mg m^{-3}) above the background can be derived from h and σ, given as $H = h/(\sigma\sqrt{2\pi})$. We define $\rho' = H/(H+B_0)$ to quantify the relative importance of the peak compared with the background. Here 197 sets of parameters of biomass profiles were archived after excluding values lying outside the range of mean $\pm$ 3 std.

2.4. Nearest Neighbor Method and local algorithm of primary production

To estimate primary production from remote sensing, we need to assign, for every pixel in the remotely sensed chlorophyll field, the parameters of the photosynthesis response and the parameters for the vertical distribution of chlorophyll. Here, the archived data on these parameters acquire central importance. They can be seen as vectors whose elements are day number t, surface biomass B, surface temperature T, and parameters α^B, P_m^B, B_0, h, σ, z_m. We use the NNM for parameter assignment that searches the archives for observations made near the values of surface temperature and chlorophyll (as determined by remote sensing) for the location and date of the pixel concerned (Platt et al., 2008). The assignment of the parameters for a pixel in a given month is based on archived data from the previous, current and following months, and the averaged value of 10 nearest neighbors is assigned to each satellite pixel. The NNM supplies the first-order estimates of the parameters for each pixel. Using this method of parameter assignment, we can now apply the local algorithm to calculate the primary production for the domain of interest through the period of availability of remotely sensed data on ocean color.

The local algorithm of primary production model combines the spectral model of submarine light (Sathyendranath and Platt, 1988) with a model of the spectral response of algal photosynthesis (Platt and Sathyendranath, 1988; Sathyendranath et al., 1989). It calculates primary production as a function of depth z

$$P(z) = \frac{B(z)\prod(z)}{\sqrt{1+(\prod(z)/P_m^B)^2}}, \quad (2)$$

with

$$\prod(z) = \sec\theta \int \alpha^B(z,\lambda) I_d(z,\lambda,\theta)\, d\lambda + 1.2 \int \alpha^B(z,\lambda) I_s(z,\lambda)\, d\lambda, \quad (3)$$

where the direct sunlight I_d and the diffuse sky light I_s are computed from the spectral model of underwater light field (Sathyendranath and Platt, 1988), λ is the wavelength ranging from 400 and 700 nm, and θ is the in-water zenith angle. The spectral shape of $\alpha^B(\lambda)$ is given and its magnitude is scaled by α^B (Sathyendranath et al., 1989). The daily water-column production is the integral of $P(z)$ through the photic zone and over the entire day.

2.5. A model to characterize phytoplankton seasonality

Our previous work on phytoplankton phenology has concentrated on the application of a single-peak Gaussian model to spring blooms (Zhai et al., 2011). For generality, it is desirable to extend the period of interest to include possible summer or fall blooms. To accomplish this, we applied a new function, namely a two-peak Gaussian model

$$B(t) = B_B + \beta t + a_1 \exp\left[-\frac{(t-t_{m_1})^2}{2\sigma_1^2}\right] + a_2 \exp\left[-\frac{(t-t_{m_2})^2}{2\sigma_2^2}\right] \quad (4)$$

to define objectively the characteristics of phytoplankton blooms over the entire year. Here B_B (mg m^{-3}) is the background value of chlorophyll concentration, a_1 and a_2 (mg m^{-3}) are the bloom amplitudes, σ_1 and σ_2 (day) define the width of the chlorophyll peaks, and t_{m_1} and t_{m_2} (day) define the time at which the maximum of bloom occurs. The linear term βt (mg m^{-3}), where β (mg m^{-3} week^{-1}) is a parameter that defines the rate of decrease (increase) of chlorophyll concentration with time from March to October. The optimal values of eight parameters were determined by the genetic algorithm, a search technique to find solutions for global optimization problems (Zhai et al., 2011). The initiation of the bloom is a useful indicator and can be derived from the initial parameters of the two-peak Gaussian function. It is defined in relative terms as the time when the chlorophyll concentration reaches 20% of the amplitude of the bloom.

3. Results and discussion

3.1. Variability of P–I and profile parameters

To examine how the oceanographic differences in the provinces are reflected in the structure of the parameters of photosynthetic–light curve and biomass profile, we averaged the parameters by province and by season (Table 1) and performed an analysis of variance to determine which means are significantly different from each other. In spring (April–June), the mean assimilation number was below 1.9 mg C (mg Chl)$^{-1}$ h^{-1} in Arctic and Mixed waters, which were significantly different from the values in the provinces of Atlantic, northern and southern Iceland Shelf. It is noteworthy that in spring the mean P_m^B was

Table 1
Mean values (and s.d. in parentheses) of photosynthetic parameters, assimilation number (P_m^B) and initial slope (α^B), temperature (T), and chlorophyll concentration (B) and number of stations (N) for different provinces and for the entire area in four seasons.

Region	P_m^B (mg C (mg Chl)$^{-1}$ h^{-1})	α^B (mg C (mg Chl)$^{-1}$ h^{-1} (W m^{-2})$^{-1}$)	N	T (°C)	B (mg m^{-3})	N
Spring						
Polar	2.4 (1.1)	0.26 (0.16)	11	1.8 (3.7)	2.4 (2.5)	12
Arctic	1.9 (0.9)	0.21 (0.13)	66	1.6 (1.8)	2.5 (2.8)	66
Mixed	1.4 (0.6)	0.17 (0.09)	13	4.5 (1.1)	2.1 (1.0)	13
Atlantic	2.9 (1.3)	0.25 (0.17)	30	8.2 (1.4)	1.3 (1.2)	29
N. Iceland Shelf	2.6 (1.3)	0.24 (0.13)	101	3.1 (1.4)	4.2 (4.0)	103
S. Iceland Shelf	2.9 (1.2)	0.19 (0.09)	173	6.3 (2.1)	4.4 (4.3)	179
Total	2.6 (1.2)	0.21 (0.11)	394	4.7 (1.8)	3.7 (3.7)	402
Summer						
Polar	1.9 (2.1)	0.25 (0.15)	9	1.0 (1.8)	0.6 (0.4)	10
Arctic	2.0 (0.7)	0.25 (0.17)	53	5.6 (1.7)	0.7 (1.6)	53
Mixed	–	–	–	–	–	–
Atlantic	2.4	0.38	1	10.1	1.1	1
N. Iceland Shelf	2.6 (0.8)	0.22 (0.08)	24	7.2 (1.9)	1.5 (1.0)	24
S. Iceland Shelf	3.1 (1.0)	0.28 (0.15)	16	8.6 (1.5)	2.2 (1.6)	18
Total	2.3 (1.0)	0.25 (0.14)	103	6.1 (1.1)	1.1 (1.3)	106
Fall						
S. Iceland Shelf	2.8 (0.2)	0.30 (0.03)	4	5.1 (0.3)	0.3 (0.1)	4
Total	2.8 (0.2)	0.30 (0.03)	4	5.1 (0.3)	0.3 (0.1)	4
Winter						
N. Iceland Shelf	1.85	0.21	1	–	–	–
S. Iceland Shelf	1.4 (0.3)	0.12 (0.02)	3	1.5 (0.3)	0.4 (0.09)	3
Total	1.5 (0.3)	0.14 (0.04)	4	1.5 (0.3)	0.4 (0.09)	3

2.4 mg C (mg Chl)$^{-1}$ h^{-1} in Polar water, which was not significantly different from the P_m^B in the adjacent southern Iceland Shelf and Atlantic province, because the sampling locations within the Polar province were close to the boundaries between Polar and Atlantic provinces, and were often influenced by the warm Atlantic water. In summer (July–September), the mean assimilation number was about 2.0 mg C (mg Chl)$^{-1}$ h^{-1} in the cold Arctic and Polar provinces and was significantly different from the mean value of 3.1 mg C (mg Chl)$^{-1}$ h^{-1} in southern Iceland Shelf. In fall (October–December) and winter (January–March), few observations were measured on the Iceland Shelf provinces, and the mean P_m^B decreased from 2.8 to 1.5 mg C (mg Chl)$^{-1}$ h^{-1} from fall to winter. Indeed, we found that there were positive relationships between temperature and assimilation number (r=0.24), which provide the justification to use temperature as a predictor of the assimilation number in the NNM. The values of initial slope α^B (mg C (mg Chl)$^{-1}$ h^{-1} (W m^{-2})$^{-1}$) showed weak spatial variations between provinces, and a weak seasonal cycle following the temperature.

We had fewer sets of profile parameters (N=197) than P–I parameters (N=505) available to us (Tables 1 and 2). Differences in profile parameters (Table 2) across province boundaries were slight, whereas the differences in B_{0z}, h and σ between seasons were significant. The depth of the chlorophyll maximum z_m was around 20 m in both spring and fall, and for all provinces except for the single valid observation in the Polar province in spring. The thickness of the subsurface chlorophyll layer σ was reduced; the background biomass B_{0z}, the total biomass above the background h and the height H decreased from spring to summer according to the averaged values for the whole area (Table 2). These seasonal changes of profile parameters are consistent with general knowledge of seasonal cycles of algal growth in the ocean, which serves as the rationale for the parameter assignment using the NNM.

3.2. Seasonal changes in chlorophyll concentration

Fig. 3 shows the climatology of monthly chlorophyll concentration from March to October. The high chlorophyll concentration in coastal waters around Iceland is related to surrounding water masses. The north Icelandic Shelf (Fig. 1) is characterized as a frontal zone area fed by various oceanic currents: the North Icelandic Irminger Current, the East Icelandic Current, the East Greenland Current and clockwise coastal current (Stefánsson, 1962). The shelf waters south and southwest of Iceland are formed mainly from warm, saline Atlantic water, but are diluted by fresh water from land in near shore area (Stefánsson and Gudmundsson, 1978). There was, however, relatively low chlorophyll concentration in shelf areas around Faroes, because the Faroe Shelf water is more vertically homogeneous throughout the year inside the 100 m contour where the tidal mixing is strong (Larsen et al., 2008). The chlorophyll concentration was consistently high north of the Iceland–Faroe Ridge from June to October, likely related to the replenishment of nutrients mediated by the frontal mixing of the water masses of North Atlantic Current and East Icelandic Current.

The annual chlorophyll cycle around Iceland was generally characterized by a pronounced spring peak in all provinces, with higher bloom amplitude on the Iceland Shelf than in the oceanic provinces (Fig. 4), whereas in temperate latitudes of the Northwest Atlantic, there are usually two well-developed blooms per year. Platt et al. (2009a) used a theoretical model to explain that the complex dependance of bloom frequency on latitude is related to the annual PAR forcing. The theoretical model predicts that there are two blooms in middle latitude (40–50°N), one bloom in high latitude (60–70°N) and a transition zone in between. Their model results are supported by ocean color time series of chlorophyll extracted around Iceland between 60°N and 70°N. The general latitudinal trend in the seasonality of chlorophyll concentration is often modified by the local physical forcing. For instance, a set of minor bloom peaks occurred in the Atlantic water, and two blooms were well developed on the southern Iceland Shelf. Within the shelf region south of Iceland, the spring bloom generally started in nearshore waters and was delayed with increasing distance from the coast, which was affected by the interaction between runoff and wind regime (Thordardottir, 1986).

The spring bloom is triggered by the shallowing of the mixed-layer depth, and its timing of initiation could vary by one month between different regions around Iceland. The bloom started to

Table 2
Mean values (and s.d. in parentheses) of profile parameters and total number of stations (N) for different provinces and for the entire area in spring and summer. B_0 is the background chlorophyll concentration, h determines the total biomass above the background, σ controls the thickness of the peak, z_m is the depth of the chlorophyll maximum, H is the height above the background, and $\rho' = H/(H+B_0)$ defines the relative importance of the peak compared with the background.

Region	B_0 (mg m^{-3})	h (mg m^{-2})	σ (m)	z_m (m)	H (mg m^{-3})	$H/(H+B_0)$	N
Spring							
Polar	0.07	51	33.4	7.5	0.6	0.9	1
Arctic	0.37 (0.48)	178 (202)	22.9 (14.7)	25.2 (16.8)	3.7 (3.8)	0.90 (0.10)	37
Mixed	0.10 (0.02)	61 (40)	15.0 (3.7)	16.2 (8.3)	1.8 (1.5)	0.90 (0.02)	2
Atlantic	0.19 (0.20)	244 (214)	28.1 (14.6)	21.3 (15.1)	3.9 (3.7)	0.90 (0.05)	11
N. Iceland Shelf	0.48 (0.40)	289 (298)	22.1 (17.8)	17.4 (15.6)	5.6 (3.2)	0.90 (0.05)	29
S. Iceland Shelf	0.86 (0.77)	172 (214)	15.8 (13.2)	19.7 (14.8)	5.0 (6.4)	0.80 (0.20)	66
Total	0.59 (0.65)	200 (232)	19.9 (15.0)	20.6 (15.5)	4.6 (4.8)	0.86 (0.13)	146
Summer							
Polar	0.44 (0.49)	44 (32)	8.2 (4.1)	25.1 (11.1)	2.6 (2.4)	0.84 (0.07)	6
Arctic	0.27 (0.38)	51 (37)	13.4 (8.0)	21.8 (14.2)	1.7 (1.4)	0.90 (0.10)	38
Mixed	–	–	–	–	–	–	–
Atlantic	–	–	–	–	–	–	–
N. Iceland Shelf	0.28 (0.36)	44 (47)	8.7 (3.8)	19.2 (8.7)	1.9 (1.3)	0.90 (0.10)	7
S. Iceland Shelf	–	–	–	–	–	–	–
Total	0.29 (0.39)	49 (37)	12.1 (7.4)	21.8 (13.2)	1.8 (1.5)	0.89 (0.10)	51

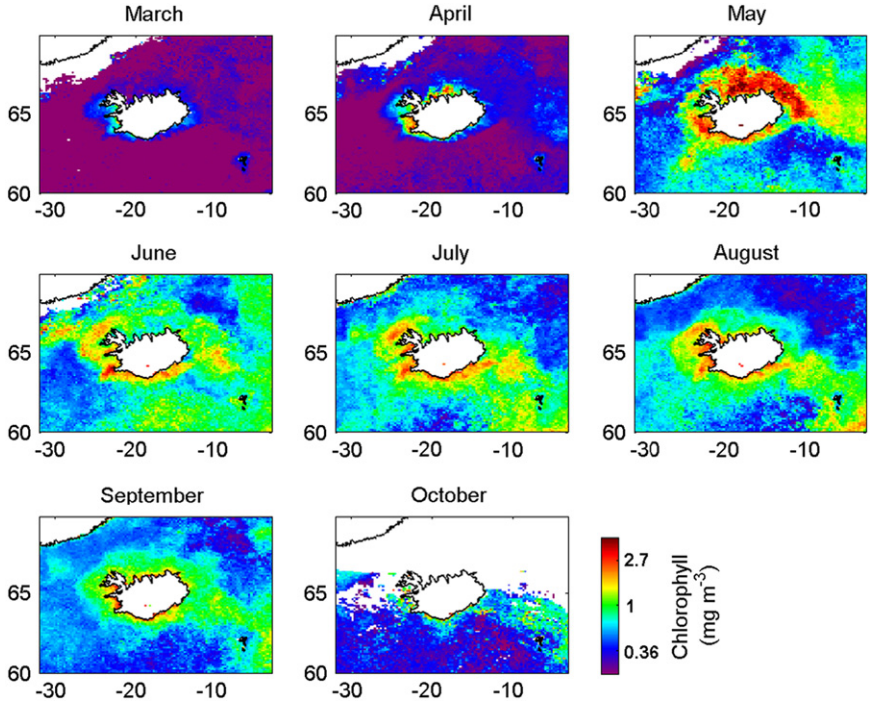

Fig. 3. Climatology of monthly chlorophyll concentration from March to October. White areas of sea surface reflect that there is no SeaWiFS data available on surface chlorophyll distribution.

develop in early April in the provinces north of Iceland, whereas the bloom did not start until mid-May in the Atlantic water and southern Iceland Shelf (Fig. 4). The differences in bloom timing between provinces are affected by the stability of water column. Fig. 5 shows that the seasonal cycles of the hydrographic structure and the mixed layer depth are significantly different between the Arctic and Atlantic waters. The Arctic water is generally cold and fresh and has a stable surface layer in comparison with the Atlantic water. In winter, the mixed layer reaches 700 m deep in the Atlantic water, whereas the Arctic water has shallower mixed layer depth of about 150 m. In spring, the increasing solar heating enhances the stratification and results in the shallower mixed-layer depth generally in the study area. The melting sea ice and fresh water run-off promote the much rapid shoaling of the mixed layer in the Arctic water, resulting in the earliest spring bloom there.

To reconcile the differences in bloom timing, we calculated the depth-averaged PAR in the mixed layer

$$\langle I \rangle_{Z_m} = \frac{I_T}{kZ_m}[1-\exp(-kZ_m)], \quad (5)$$

where k (m^{-1}) is the light attenuation coefficient, I_T (W m^{-2}) the SeaWiFS total daily PAR, and Z_m (m) the mixed-layer depth. In Sverdrup's (1953) theory, it is assumed that phytoplankton growth and loss are balanced in the mixed layer at the start of spring bloom. The averaged PAR in the mixed layer at the time of bloom initiation (Fig. 6) had a narrow range between 7 and 22 W m^{-2}, compared with the full range of the annual cycle

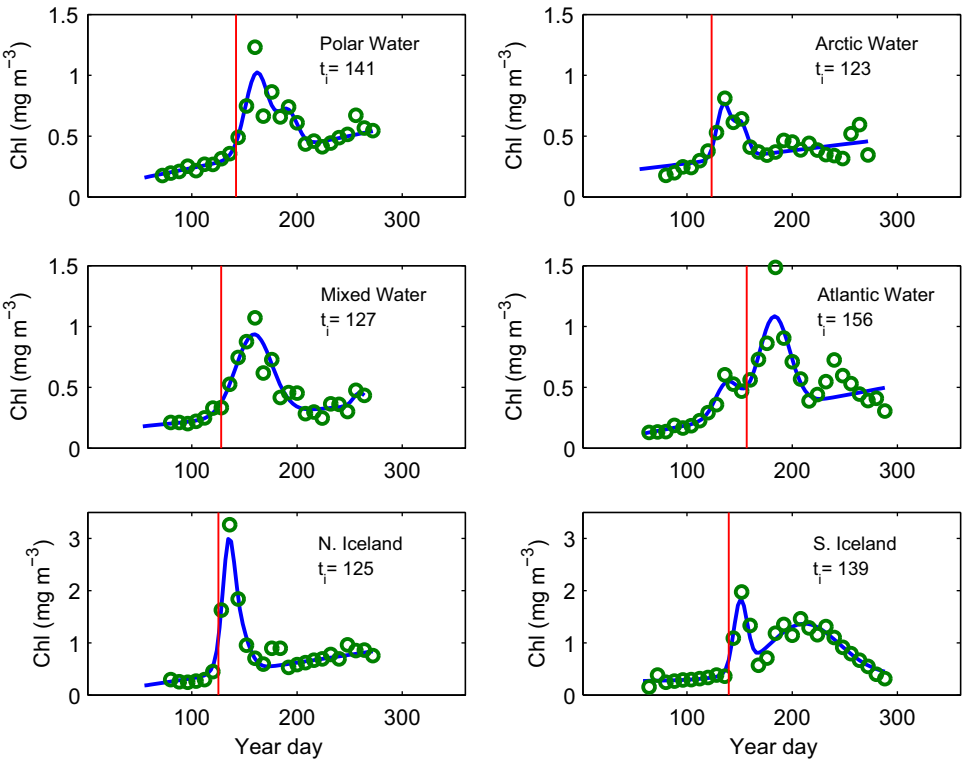

Fig. 4. Climatology of 8-day chlorophyll concentration and fitted two-peak Gaussian curve at six selected locations indicated by yellow circles in Fig. 1. The initiation of spring bloom (t_i) is indicated by the vertical line.

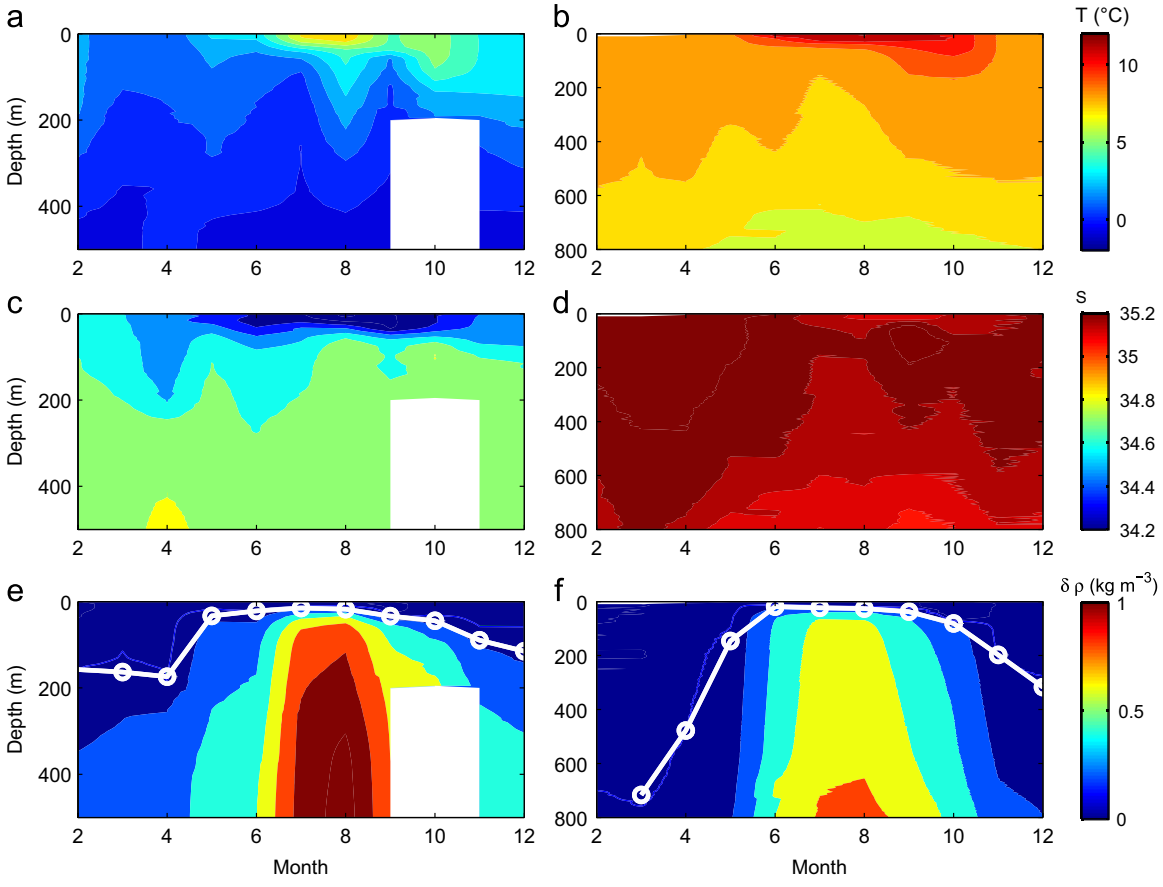

Fig. 5. (a and b) Temperature, (c and d) salinity and (e and f) density difference from the surface in the depth–time plane for Arctic water (left panels) and Atlantic water (right panels). White circled line indicates the mixed-layer depth. White box indicates no data available below 200 m in October.

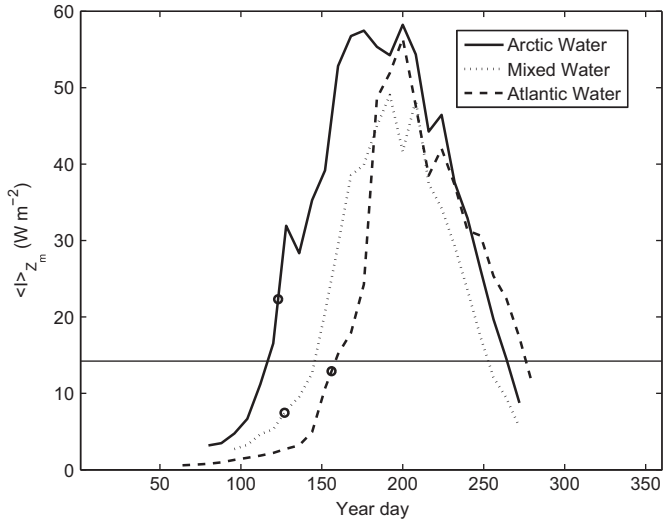

Fig. 6. Seasonal cycle of the mixed-layer averaged PAR for Arctic, Mixed and Atlantic waters. The initiation of spring bloom is marked by circles, and $\langle I \rangle_{Z_m} = 14\ \mathrm{W\,m^{-2}}$ is marked by the horizontal line.

between 0 and 60 W m^{-2}. The necessary condition for spring bloom to start is that the mixed-layer irradiance has to reach this critical value. The mean value of $\langle I \rangle_{Z_m}$ at the initiation of bloom was 14 W m^{-2}, similar to the value estimated in the temperate Northwest Atlantic (Platt et al., 2009b; Zhai et al., 2011). Henson et al. (2006) also calculated this quantity of 10.4 ± 2.1 W m^{-2} in Irminger Basin, which is lower compared with our value. This is probably because in their study the initiation of spring bloom was defined differently as the day of year when the chlorophyll concentration first rises 5% above that year's annual median.

3.3. Computation of primary production

We have calculated the primary production for each month (represented by the 15th of each month) from March to October. The climatology of monthly primary production is shown in Fig. 7 and displayed similar strong spatial patterns and seasonal cycles to the chlorophyll series. The primary production varied seasonally between 150 and 4000 mg C m^{-2} day^{-1}, with the lowest production in March and high production from May to August. The peak of primary production occurred in May in northeastern Iceland Shelf, but was delayed by a month in southwestern Iceland Shelf, coincident with the timing of bloom peak (Fig. 8). The primary production for Arctic water was generally lower than that in Atlantic water (Fig. 8). Thordardottir (1977) concluded that the magnitude of primary production is closely related to the water masses. The high *in situ* primary production was observed at stations with salinity >34.5, and low production was found in waters with salinity <34.5 in Iceland Shelf regions (Gudmundsson, 1998). The interpretation for the differences in production during the summer between Atlantic and Arctic waters (Fig. 8) could be related to the differences in hydrographic conditions (Thordardottir, 1984). Pronounced stratification in Arctic water would reduce the upward transport of nutrients, resulting in low production, whereas resupply of nutrients would be favored in Atlantic water with low stability, thus promoting phytoplankton growth (Fig. 5).

The annual primary production was derived through the integration of monthly primary production (Fig. 9). The spatial structure in the climatology of modeled annual primary production was consistent with observations made by the simulated *in situ* method using ships as a platform, but, inevitably, the fields produced from the remotely sensed data are smoother. The correlation between the estimated and simulated *in situ* primary production is 0.57, and the difference between them is about 50% of the simulated *in situ* primary production. The relatively poor retrieval of surface chlorophyll by standard processing of SeaWiFS data (OC4v4) in the study area (Gudmundsson et al., 2009) may have led to overestimation of the annual production. An overestimation of chlorophyll by remote sensing seems to be the typical case most of the time, except during the Spring (Gudmundsson et al., 2009). The modeled primary production shows similar spatial pattern to the simulated *in situ* primary production: higher production on the southwestern than northeastern Iceland Shelf, and decreasing primary production in the offshore direction. The annual primary production (Table 3) was about 309 g C m^{-2} year^{-1} in the southern Iceland Shelf and 251 g C m^{-2} year^{-1} in the northern Iceland Shelf. The low production was found in the Polar and Arctic provinces, and the spatial means and standard deviations were 133 ± 49 and 179 ± 36 g C m^{-2} year^{-1} respectively. The annual production for the Mixed and Atlantic waters were 211 and 238 g C m^{-2} year^{-1} respectively.

3.4. Error analysis

The parameter assignment is a key step in computing the primary production. To assess the agreement between the assigned and the measured parameters, we evaluated the parameter assignment through its influence on the estimation of primary production (Platt et al., 2008). The reference primary production was established for the 172 stations at which both photosynthetic parameters and vertical profile were measured and was calculated with a spectral model (Platt and Sathyendranath, 1988) using the observed photosynthesis parameters, observed biomass profiles, satellite chlorophyll and clear-sky spectral irradiance with the correction of observed cloud cover. We then estimated all required parameters by the NNM using satellite chlorophyll and sea-surface temperature as inputs for each station, and calculated primary production again, using these parameters. The difference between these estimates and the reference values is caused only by the errors associated with parameter assignment. We found that the correlation between the estimates and the reference production (Fig. 10) was 0.61 ($p<0.01$), and the mean relative difference between them was 5% for all stations. The mean primary production estimated by NNM in August (Table 4) had the largest error and was about 80% higher than the reference value, possibly associated with the fewer observations of chlorophyll profiles in August and adjacent months in the *in situ* database.

A deep chlorophyll maximum (DCM) is a common feature of pigment profiles, especially in summer when the water column is strongly stratified, and the chlorophyll concentration at the surface is low (Table 2). Therefore to examine the effect of DCM on the water column primary production, we calculated the production for a simple case of uniform biomass, in which $B(z)$ is equal to satellite chlorophyll and other set-up of spectral model is identical to that outlined in Section 2. The seasonal cycle of daily water column primary production for the uniform biomass case (Fig. 8) followed the surface chlorophyll more closely compared with that for the non-uniform biomass case. The difference in production between them was of little significance from March to May but was relatively large after June, because the pigments are distributed near-uniformly in the upper water column in spring and have a strong DCM in summer. The annual production for the uniform biomass case (Fig. 11) is consistently lower than that for the non-uniform case. After integration over the study area, the vertically uniform model tended to underestimate annual production by 36%. Platt and Sathyendranath (1991) found that the uniform model gave an error of 20% for the Atlantic between 20°S and 70°N, and a larger error in the shelf subarctic region.

Platt and Sathyendranath (1991) suggested that the non-spectral model could perform almost as well as the spectral

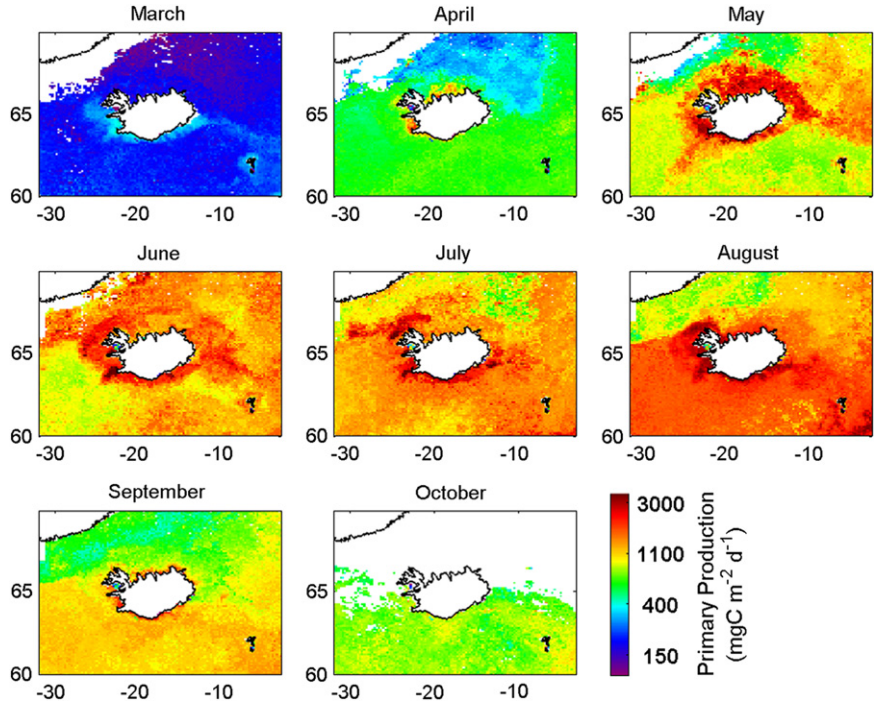

Fig. 7. Climatology of monthly primary production from March to October. White areas of sea surface reflect that there is no SeaWiFS data available on surface chlorophyll distribution.

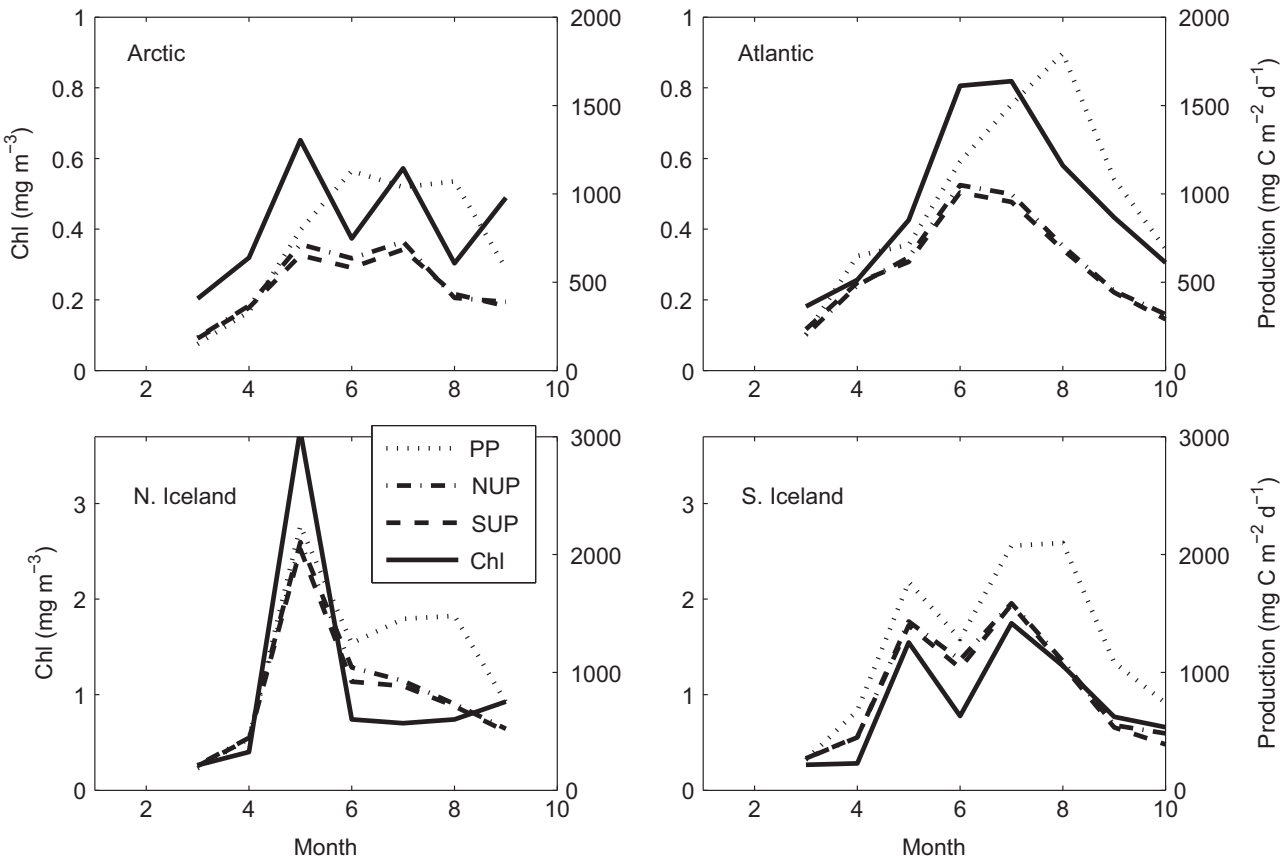

Fig. 8. Seasonal cycle of chlorophyll concentration (solid line) and primary production estimated from ocean color data at four selected locations. The production (PP) calculated by the spectral, non-uniform biomass model is indicated by the dotted line; the production (SUP) calculated by the spectral, uniform biomass model is indicated by the dashed line; the production (NUP) calculated by the non-spectral, uniform biomass model is indicated by the dash-dotted line.

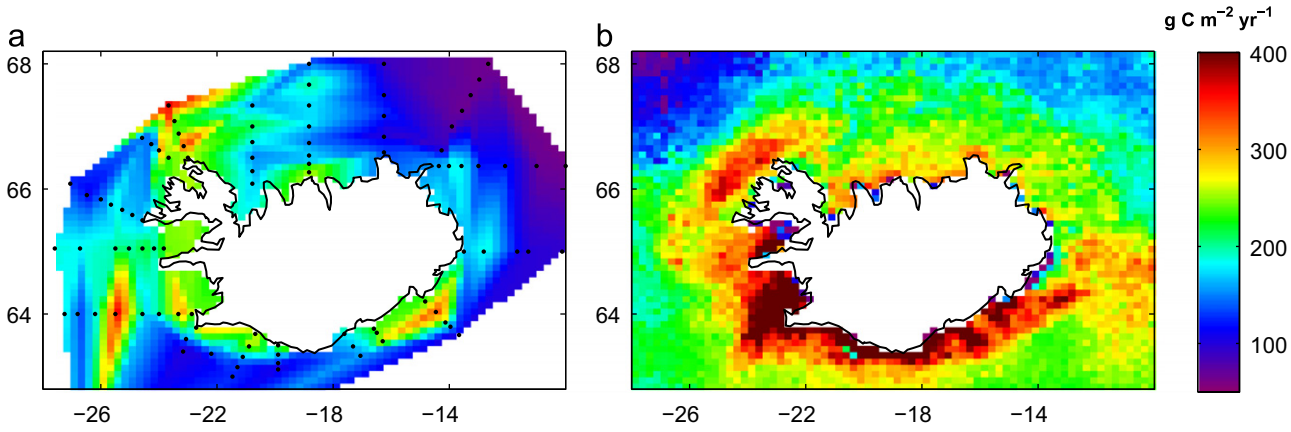

Fig. 9. (a) Annual primary production estimates at fixed stations, based solely on *in situ* data during 1958–1982 and (b) primary production through water column, calculated using Nearest Neighbor Method, for period from March to October. Fig. 9(a) is redrawn from Thordardóttir (1994).

Table 3
Mean values (± s.d.) of annual primary production for six provinces.

Province	Primary production ($g\,C\,m^{-2}\,year^{-1}$)
Polar water	133 ± 49
Arctic water	179 ± 36
Mixed water	211 ± 20
Atlantic water	238 ± 22
N. Iceland Shelf	251 ± 41
S. Iceland Shelf	309 ± 81
Total	220 ± 57

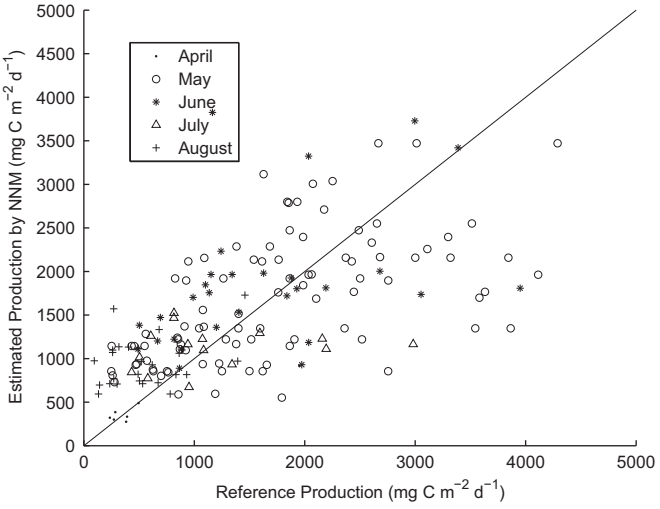

Fig. 10. Reference primary production vs. estimated production by NNM at stations where both *P–I* and profile parameters were sampled.

Table 4
Mean values (and s.d. in parentheses) of reference primary production and primary production estimated by NNM and total number of stations (*N*) from April to August.

	Reference ($mg\,C\,m^{-2}\,day^{-1}$)	Estimated by NNM ($mg\,C\,m^{-2}\,day^{-1}$)	*N*
April	573 (613)	431 (225)	7
May	1789 (1057)	1685 (725)	94
June	1628 (895)	1860 (783)	29
July	1205 (732)	1117 (239)	15
August	552 (356)	957 (281)	26
Total	1473 (1024)	1503 (743)	171

model, provided that the light attenuation coefficient were tuned with care. To demonstrate this consistency, we also ran the non-spectral model forced by SeaWiFS PAR with homogeneous biomass profile specified according to satellite chlorophyll. The daily integral of photosynthesis is given by Platt and Sathyendranath (1993)

$$P_{z,T} = \frac{BP_m^B D}{K} f(I_*^m), \tag{6}$$

where D is day length, attenuation coefficient K is derived from a lookup table of K against B computed for the photic zone using the spectral model of submarine light (Sathyendranath and Platt, 1988), $I_*^m = \pi I_T/(2DI_k)$, and I_T is SeaWiFS total daily PAR. The values of function $f(I_*^m)$ were tabulated by Platt and Sathyendranath (1993) for the range $0.2 < I_*^m < 20$, and are retabulated to cover a wide range $0 < I_*^m < 50$ in our study, given in Table 5. The seasonal cycle of production calculated by function (6) is generally in agreement with that calculated by the spectral, uniform biomass model (Fig. 8). The non-spectral model yielded annual production values slightly larger than those from the spectral uniform model by 3% for the study area. The use of non-linear relation between K and B did not eliminate the difference between spectral and non-spectral models, since the light is strongly attenuated at the surface due to the high absorption of red light by pure seawater.

4. Conclusion

In this study, we demonstrated that satellite data provide valuable tools for studying phytoplankton phenology and estimating primary production in Iceland–Faroe region. Our results are consistent with knowledge gained from the conventional research methods based on cruises, and also reveal detailed information on seasonal changes in phytoplankton biomass and production, which could not be achieved by ship sampling at the same temporal and spatial scales. We also showed the applicability and validity of the NNM to the Iceland–Faroe region as an operational tool to estimate primary production.

Our results reveal that the spatial distribution and seasonal cycle of biomass and production in the study region are controlled by the water masses with different hydrographic features. The spring bloom is the salient feature of seasonality of phytoplankton, and its initiation time varies between provinces. The early spring bloom in Arctic water and delayed one in Atlantic water are associated with the strong and weak stratification of water column in spring respectively. The annual primary production exhibits strong inhomogeneity around Iceland, with high values

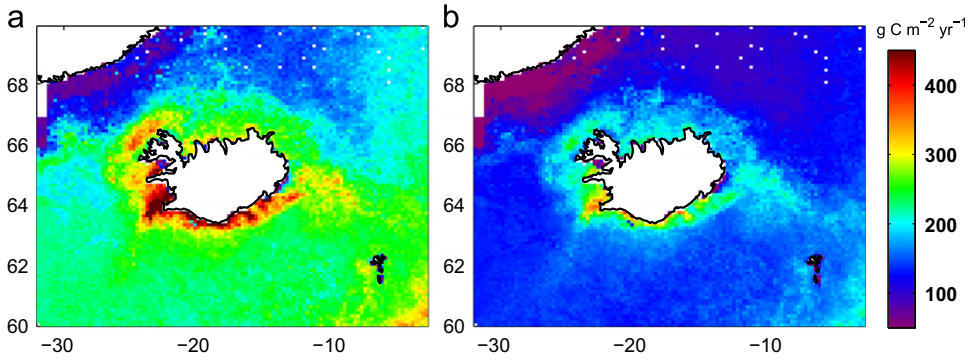

Fig. 11. Primary production integrated for period from March to October calculated using (a) spectral, non-uniform biomass model and (b) spectral, uniform biomass model.

Table 5
Tabulated values for the canonical function, $f(I_*^m)$. I_*^m is the dimensionless, surface irradiance at local noon.

I_*^m	$f(I_*^m)$	I_*^m	$f(I_*^m)$	I_*^m	$f(I_*^m)$
0.0	0.0000	17.0	2.7547	34.0	3.4291
1.0	0.5318	18.0	2.8098	35.0	3.4576
2.0	0.9137	19.0	2.8620	36.0	3.4852
3.0	1.2036	20.0	2.9116	37.0	3.5122
4.0	1.4336	21.0	2.9589	38.0	3.5384
5.0	1.6229	22.0	3.0040	39.0	3.5639
6.0	1.7831	23.0	3.0472	40.0	3.5888
7.0	1.9216	24.0	3.0886	41.0	3.6131
8.0	2.0435	25.0	3.1284	42.0	3.6369
9.0	2.1523	26.0	3.1666	43.0	3.6600
10.0	2.2505	27.0	3.2035	44.0	3.6827
11.0	2.3400	28.0	3.2390	45.0	3.7049
12.0	2.4221	29.0	3.2733	46.0	3.7265
13.0	2.4981	30.0	3.3065	47.0	3.7477
14.0	2.5686	31.0	3.3386	48.0	3.7685
15.0	2.6346	32.0	3.3697	49.0	3.7889
16.0	2.6965	33.0	3.3998	50.0	3.8088

Fig. 12. Thorunn Thordardottir (1925–2007). Photo from the collection of the Marine Research Institute, Iceland.

on the southern Iceland Shelf and low production on the northern Iceland Shelf. It is regulated by the vertical nutrient transport to the surface, which is enhanced in weakly stratified Atlantic water than in strongly stratified Arctic water.

The information on phytoplankton growth will be utilized in analyzes of data on survival and growth of grazers and survival and changes in the biomass of predators (fishes) and benthic scavengers. One of our basic goals is to acquire understanding of the causes to variations in harvestable marine organisms and to advise the managers on related marine ecological issues. Given the appropriate data, we may be able to reveal the significant correlations between phytoplankton growth and the fate of the primary production through the food chain and elucidate the principal causes for changes. Understanding of the principles governing the regional development of phytoplankton growth, and the relevant empirical correlations, may in turn help us to argue for rational decisions in marine stewardship.

Acknowledgments

This work is dedicated to the memory of Thorunn Thordardottir (1925–2007), pioneer of phytoplankton dynamics around Iceland, and a much-valued colleague (Fig. 12). We thank Héðinn Valdimarsson for making hydrographical data available and for relevant comments, Ellie Doggett and Marie-Hélène Forget for help in collating the archived database. This work was funded by the Canadian Space Agency under the GRIP programme. This work is also a contribution to the Ocean 2025 and NCEO programmes of NERC (UK) and to the CoastColour and OC-CCI projects of ESA.

References

Anon, 2008. Environmental Conditions in Icelandic Waters 2007. MRI report series, 139, pp. 14–17.

Astthorsson, O.S., Gislasona, A., Jonsson, S., 2007. Climate variability and the Icelandic marine ecosystem. Deep-Sea Research 54, 2456–2477.

Boyer, T.P., Antonov, J.I., Baranova, O.K., Garcia, H.E., Johnson, D.R., Locarnini, R.A., Mishonov, A.V., Seidov, D., Smolyar, I.V., Zweng, M.M., 2009. World ocean database 2009. In: Levitus, S. (Ed.), NOAA Atlas NESDIS 66. U.S. Gov. Printing Office, Washington, DC, pp. 216. (DVDs).

Ferraro, R.R., Weng, F., Grody, N.C., Basist, A., 1996. An eight-year (1987–1994) time series of rainfall, clouds, water vapor, snow cover, and sea ice derived from SSM/I measurements. Bulletin of the American Meteorological Society 77, 891–905.

Gudmundsson, K., 1998. Long-term variation in phytoplankton productivity during spring in Icelandic waters. ICES Journal of Marine Science 55, 635–643.

Gudmundsson, K., Valsdóttir, K.J., 2004. Frumframleidnimlingar á Hafrannsóknastofnuninni árin 1958–1999 (Primary Productivity Measurements at the Marine Research Institute in Iceland, 1958–1999). MRI report series, 107, 56 pp (in Icelandic).

Gudmundsson, K., Heath, M.R., Clarke, E.D., 2009. Average seasonal changes in chlorophyll a in Icelandic waters. ICES Journal of Marine Science, 2133–2140.

Henson, S.A., Robinson, I.S., Allen, J.T., Waniek, J.J., 2006. Effect of meteorological conditions on interannual variability in timing and magnitude of the spring bloom in the Irminger Basin, North Atlantic. Deep-Sea Research Part I 53, 1601–1615.

Jassby, A.D., Platt, T., 1976. Mathematical formulation of the relationship between photosynthesis and light for phytoplankton. Limnology and Oceanography 21, 540–547.

Larsen, K.M.H., Hansen, B., Svendsen, H., 2008. Faroe shelf water. Continental Shelf Research 28, 1754–1768.
Miller, P.I., 2009. Composite front maps for improved visibility of dynamic oceanic fronts on cloudy AVHRR and SeaWiFS data. Journal of Marine Systems 78, 327–336.
Parsons, T.R., Maita, Y., Lalli, C.M., 1984. A Manual of Chemical and Biological Methods for Seawater Analysis. Pergamon Press, Oxford.
Platt, T., Gallegos, C.L., Harrison, W.G., 1980. Photoinhibition of photosynthesis in natural assemblages of marine phytoplankton. Journal of Marine Research 38, 687–701.
Platt, T., Sathyendranath, S., 1988. Oceanic primary production—estimation by remote sensing at local and regional scales. Science 241, 1613–1620.
Platt, T., Sathyendranath, S., Caverhill, C., Lewis, M., 1988. Ocean primary production and available light: further algorithms for remote sensing. Deep-Sea Research Part I 35, 855–879.
Platt, T., Sathyendranath, S., 1991. Biological production models as elements of coupled, atmosphere-ocean models for climate research. Journal of Geophysical Research 96, 2585–2592.
Platt, T., Sathyendranath, S., 1993. Estimators of primary production for interpretation of remotely sensed data on ocean color. Journal of Geophysical Research 98, 14561–14576.
Platt, T., Sathyendranath, S., Fuentes-Yaco, C., 2007. Biological oceanography and fisheries management: perspective after 10 years. ICES Journal of Marine Science 64, 863–869.
Platt, T., Sathyendranath, S., Forget, M.-H., White III, G.N., Caverhill, C., Bouman, H., Devred, E., Son, S., 2008. Operational estimation of primary production at large geographical scales. Remote Sensing of Environment 112, 3437–3448.
Platt, T., White III, G.N., Zhai, L., Sathyendranath, S., Roy, S., 2009a. The phenology of phytoplankton blooms: ecosystem indicators from remote sensing. Ecological Modelling, doi:10.1016/j.ecolmodel.2008.11.022.
Platt, T., Sathyendranath, S., White III, G.N., Fuentes-Yaco, C., Zhai, L., Devred, E., Tang, C., 2009b. Diagnostic properties of phytoplankton time series from remote sensing. Estuaries and Coasts 33, 428–439.
Sathyendranath, S., Platt, T., 1988. The spectral irradiance field at the surface and in the interior of the ocean: a model for applications in oceanography and remote sensing. Journal of Geophysical Research 93, 9270–9280.
Sathyendranath, S., Platt, T., Caverhill, C.M., Warnock, R.E., Lewis, M.R., 1989. Remote sensing of oceanic primary production: computations using a spectral model. Deep-Sea Research 36, 431–453.
Stefánsson, U., 1962. North Icelandic waters. Rit Fiskideildar 3, 1–269.
Stefánsson, U., Gudmundsson, G., 1978. The freshwater regime of Faxaflói, Southwest Iceland, and its relationship to meteorological variables. Estuarine and Coastal Marine Science 6, 535–551.
Steemann Nielsen, E., 1952. The use of radioactive carbon (C^{14}) for measuring organic production in the sea. Journal du Conseil, Conseil International pour l'Exploration de la Mer 18, 117–140.
Strickland, J.D.H., Parson, T.R., 1972. A practical handbook of seawater analysis. Fisheries Research Board of Canada, Bulliten 167.
Sverdrup, H.U., 1953. On conditions for the vernal blooming of phytoplankton. Journal du Conseil, Conseil International pour l'Exploration de la Mer 18, 287–295.
Theodorsson, P., 1975. The study of 14-C penetration into filters in primary productivity measurements using double side counting. Limnology and Oceanography 20, 288–291.
Theodorsson, P., 1984. Penetration Correction of Geiger Counting and on Board Determination of Primary Productivity. ICES C.M., 1984/L:18.
Thordardottir, Th., 1977. Primary production in North Icelandic waters in relation to recent climatic changes. In: Dunbar, M.J. (Ed.), Polar Oceans, Proceedings of the Polar Oceans Conference, McGill University, Montreal, May 1974. Arctic Institute of America, China, pp. 655–665.
Thordardottir, Th., 1984. Primary Production North of Iceland in Relation to Water Masses in May–June 1970–1989. International Council for the Exploration of the Sea CM 1984/L:20, 17 pp.
Thordardottir, Th., 1986. Timing and duration of spring blooming south and southwest of Iceland. In: Skreslet, S. (Ed.), The Role of Freshwater Outflow in Coastal Marine Ecosystems NATO ASI Series, vol. G7. Springer, Berlin, pp. 345–360.
Thordardottir, Th., 1994. Plöntusvif og frumframleidni í sjónum vid Ísland (Phytoplankton and primary production in Icelandic waters). In: Stefansson, U. (Ed.), Islendingar, hafid og audlindir thess (Icelanders, the Ocean and Its Resources). Societas Scientarium Islandica, Reykjavik, pp. 65–88. (in Icelandic).
Zhai, L., Platt, T., Tang, C., Sathyendranath, S., Hernández Walls, R., 2011. Phytoplankton phenology on the Scotian Shelf. ICES Journal of Marine Science. doi:10.1093/icesjms/fsq175.